







Starch from quinoa and amaranth flour for potential food applications: Thermal, electrokinetic and spectral characterization of the water-based starch extract

 **Jane Tafadzwa Muchekeza**^{1,2*}

 **Komeine Kotokeni Mekondjo Nantanga**¹

 **Theopoline Omagano Itenge**³

 **Mambo Moyo**⁴

¹Department of Food Science and Systems, School of Agriculture & Fisheries Sciences, University of Namibia, Namibia.

^{1,2}Email: muchekezaj@staff.msu.ac.zw

¹Email: knantanga@unam.na

²Department of Animal and Wildlife Sciences, Midlands State University, P Bag 9055, Gweru, Zimbabwe.

³Department of Animal Production, Agribusiness and Economics, School of Agriculture & Fisheries Sciences, University of Namibia, Namibia.

³Email: tamushendje@unam.na

⁴Department of Chemical Sciences, Midlands State University, P Bag 9055, Gweru, Zimbabwe.

⁴Email: moyom@staff.msu.ac.zw



(+ Corresponding author)

ABSTRACT

Article History

Received: 13 June 2025

Revised: 30 September 2025

Accepted: 26 November 2025

Published: 29 December 2025

Keywords

Chemical properties

Functional Foods

Gelatinization

Pseudo cereals

Starch

Water extracted.

Quinoa and amaranth are pseudo-cereals suitable as cereal alternatives due to their potential use in functional foods. The study investigated the physicochemical properties of quinoa, amaranth, and water-extracted starches. Characterization of the flours and starches was performed using electrochemical analysis, differential scanning calorimetry, thermogravimetric analysis, powder X-ray diffraction, UV-Vis spectrometry, and Fourier Transform Infrared spectroscopy. The electrochemical analysis results indicated that extracted starches and flours are suitable electron acceptors in fermented foods. Thermal analysis by differential scanning calorimetry showed endothermic peaks of AMF (92.70 °C) > AMS (90.52 °C) > QF (84.83 °C) > CS-WFM (83.56 °C) > QS (70.41 °C), which depicted a variation in gelatinization temperatures. Fourier transform infrared spectroscopy analysis showed bands similar for all starches and flours. X-ray diffraction analysis of the powder showed different crystallinity patterns, indicating the presence of an A-type crystalline structure. UV-Vis spectrophotometry displayed peaks of 337 and 341 nm for amaranth and quinoa starch, respectively, and the quinoa peak is similar to a wide peak (340–354 nm) demonstrated by corn starch (reference). The results underline the diverse properties of quinoa, amaranth, and corn starch and indicate their potential as functional ingredients in various food applications.

Contribution/Originality: This study is one of the few investigations that have explored the novel application of electrochemical analysis combined with thermal profiling to evaluate water-extracted quinoa and amaranth starches. It provides insights into their functional potential as alternative starch sources, an approach not previously reported in starch characterization for meat product development.

1. INTRODUCTION

Amaranth (*Amaranthus hypochondriacus*) and quinoa (*Chenopodium quinoa Willd*) are Andean pseudo-cereals that are suitable alternatives to corn starch because of their potential in functional foods (Jan, Hussain, Naseer, & Bhat, 2023). The nutritional profile of the crops makes them an invaluable supplement to various dishes. They can be cooked similarly to rice or used as substitutes for wheat in baking or maize starch in meat products, thereby mitigating

reliance on crops that require expensive inputs (Balakrishnan & Schneider, 2022). Quinoa's adaptability to different climates has rendered it an essential component of Controlled Ecological Life Support Systems (CELSS) on long-duration space missions, providing vital resources such as food, oxygen, and water (Tang & Tsao, 2017). Amaranth, similar to quinoa, has been cultivated in various climates (Aderibigbe et al., 2022), including the African continent.

Quinoa and amaranth, like cereals, can be incorporated into various food products and can positively contribute to improving food security.

According to the FAOSTAT (2020) small grains such as amaranth, quinoa, and millet have the potential to significantly address global food insecurity in the context of climate change. The production and consumption of small grains can reduce overreliance on a few cereals (maize, wheat, and rice), which are insufficient to meet the global caloric requirements (FAOSTAT, 2020). Jan et al. (2023) reported that dependence on limited crops threatens food and nutritional security. Increasing crops contributing to food and nutritional security has motivated several governments and researchers to allocate resources and effort toward promoting underutilized crops as viable alternatives to common cereals (Pirzadah & Malik, 2020). Studies on the characterization of quinoa and amaranth flours and starches as alternatives to corn starch, which could potentially alleviate the heavy reliance on maize, the primary source of corn starch, are limited.

Characterization of starch extracted through the alkali wet milling process, as well as the flours, has been conducted using various analytical techniques, such as differential scanning calorimetry (DSC), thermogravimetric analysis (TGA), powder X-ray diffraction (PXRD), and Fourier transform infrared spectroscopy (FTIR) (Dong et al., 2021; Orlova & Aider, 2021; Perez-Rea & Antezana-Gomez, 2024; Sindhu & Khatkar, 2016; Torres-Vargas, García-Salcedo, & Ariza-Calderón, 2018).

However, these analyses have been conducted separately for the starches and flours rather than systematically. Jan, Panesar, Rana, and Singh (2017) also conducted FTIR analysis exclusively for quinoa water-extracted starch without employing other analytical techniques. In contrast, studies on the analysis of amaranth flour and its water-extracted starch using the aforementioned analytical techniques are lacking.

The physicochemical properties of quinoa and amaranth flours and starches, such as thermal and pasting characteristics, are influenced by their distinct starch structures and non-starch components (Valdez-Arana, Steffolani, Repo-Carrasco-Valencia, Pérez, & Condezo-Hoyos, 2020). The starch extraction method also affects these structures and components. Currently, the alkali extraction method is the predominant technique employed for starch extraction, and extensive studies have been conducted to analyze starches derived via this method. This underscores the need to comprehensively analyze starches extracted without solvents using the aforementioned analytical techniques.

Additionally, UV-Vis spectrometry has been applied only to amaranth flour to detect starch spectra. Therefore, analyzing the water-extracted starch from amaranth and quinoa flours, as well as their flours, is important because UV-Vis spectrometry provides insights into the molecular interactions and structural properties of starches, which can enhance food quality and stability (Balakrishnan & Schneider, 2022). Furthermore, systematic electrochemical analysis using cyclic voltammetry for amaranth and quinoa flours and starches has not been reported, despite its importance in highlighting the impact of starch on charge transfer (Hernandez-Jaimes et al., 2015). Charge transfer interactions between amylose in starch and meat proteins affect the stability of the protein network in meat products, consequently impacting the texture, firmness, and overall quality of the product (Scott & Awika, 2023).

This study aimed to characterize quinoa and amaranth flour and their solvent-free extracted starches, using thermal, electrokinetic, and spectral methods. The aim is to address the knowledge gap regarding the properties of water-extracted starches compared to their flours and their expected behavior when used in various thermally treated foods, including meat products. These findings will influence the future use of starch from quinoa and amaranth flours in food development.

2. MATERIALS AND METHODS

2.1. Raw Materials

Corn starch was sourced from WFM Starch Products Company, South Africa. Amaranth flour and quinoa grains were acquired from Four Season Foods Company, Zimbabwe.

2.2. Flour Preparation

Prior to analysis, the quinoa grains underwent mechanical processing. They were first dehulled using a mortar and pestle, then soaked in warm water overnight to remove saponins. After soaking, the grains were thoroughly washed and sun-dried. The dried grains were ground into flour using a Hamilton Beach HBF500S-CE laboratory blender. The milled quinoa and the purchased amaranth flour were sieved using a 500 μm sieve (universal sieve). The corn starch was also sieved with a 500 μm sieve for control purposes.

2.3. Starch Extraction

Quinoa and amaranth starches were extracted using a modified method by Jan et al. (2017). The flours were soaked in water at a 1:6 ratio at 4°C for 24 hours in a shaking incubator (Bio base -BJPX-100B). The mixture was then wet-milled for 2 minutes using a laboratory blender and passed through 250, 75, and 45 μm sieves. The resulting filtrate was centrifuged (Bio base -BKC-TH16) at 5500 rpm for 15 minutes, with the supernatant discarded and a yellowish layer of approximately 1 mm above the starch cake removed. The starch cake was repeatedly suspended in water and centrifuged four times. The starch was dried at 40°C for 12 hours in an oven (Scientific South Africa-225) and stored in sealed plastic containers at room temperature (24 to 26°C) until analysis.

2.4. Analysis of Flours and Starch

Quinoa and amaranth flours, starches, and corn starch were characterized using various types of equipment. For electrochemical experiments, an Autolab Potentiostat Galvanostat (PGSTAT 302 F) equipped with NOVA electrochemical system processing software version 1.10 was used. Briefly, 5 mg samples of each flour were dispersed in 5 mL of DMF and ultrasonicated for 30 minutes. Approximately 5 μL of the sample solution was dropped onto the bare GE and dried in an oven at 50°C for 5 minutes. The electroactive behavior was evaluated in a 5 mM potassium ferricyanide solution. The cyclic voltammetry (CV) experiment was performed by running the bare and the modified electrodes in potassium ferricyanide within the potential window of -0.2 to 0.6 V at a scan rate of 100 mVs⁻¹.

A measure of the heat flow associated with phase transitions in quinoa and amaranth flours and starches as a function of temperature was conducted using the DSC. Samples of flour and starches, weighing 5.6 mg \pm 0.5, were placed in aluminium crucibles, and water was added up to 80% moisture. Three milligrams of the flour and starch were then placed in a DSC aluminium pan. DSC experiments were performed using a TA Discovery Instrument DSC-25, with a heating rate of 10 °C min⁻¹ within a 25–150 °C temperature range under a dry nitrogen purge gas flow of 50 mLmin⁻¹.

A TGA method was employed to determine the decomposition temperature. Flour or starch (3 mg) was placed in an aluminium pan. The TA Discovery Instrument TA-550 was used with a heating rate of 10 °C min⁻¹ over a 25–450 °C temperature range, and a dry nitrogen purge gas flow was maintained at 50 mL min⁻¹.

The samples were analyzed in the 400–4000 cm⁻¹ range using a Perkin–Elmer Fourier Transform Infrared spectrophotometer (FTIR) Thermo-Scientific Nicolet 6700 for functional groups. Starch and flour samples (2 mg) were mixed with 200 mg of dried potassium bromide (KBr) powder to form a pellet, which was used for analysis.

Powder diffraction measurements were performed on a Bruker D2 Phaser 2nd Gen diffractometer using Cu K α radiation (λ = 1.5406 Å) at 298 K. The ground samples were placed on a zero-background sample holder and scanned over a 2 θ range of 5° to 60° at a scanning rate of 0.017°/s. X-rays were generated using a current of 10 mA and a

voltage of 30 kV. Crystallinity was determined by calculating the area under the specific peaks compared to the total graph area using Origin Lab software.

For UV-Vis Spectrophotometric, sample preparation was done according to Bahdanovich, Axelrod, Khlystov, and Samburova (2022). The 0.2% iodine reagent (I_2/KI) was prepared. Flour or starch (1 g) was heated at 105°C for 24 hours, following the temperature optimization by Noranizan, Dzulkifly, and Russly (2010). The starch was kept in a desiccator with sodium hydroxide (NaOH) pellets until ready for use. A 10 mg sample of desiccated flour or starch was hydrated using 0.1 mL of 95% ethanol and 1 mL of 1N NaOH solution in a 10 mL volumetric flask. The prepared sample mixture was refrigerated for 24 hours at 4 °C. The volume was adjusted to 10 mL with distilled water at the same temperature, and the solutions were refrigerated for 16–18 hours. Finally, the stock concentration was analyzed using the UV-VIS Spectrophotometer (Specord® 200 Plus) from Analytik Jena after adding 2 mL potassium triiodide. A blank sample was prepared with 0.1 mL of ethanol and 1 mL of NaOH, then adjusted to 10 mL with water.

3. RESULTS AND DISCUSSION

3.1. Electrochemical Studies

The electrochemical properties of starches and flours deposited on the gold electrode were investigated in a redox probe. Figure 1 shows cyclic voltammograms of the ferro/ferricyanide redox couple measured at bare gold, QS, AMS, CS-WFM, QF, and AMF in 5 mM potassium ferricyanide. The peak current (I_p) decreased because of the anodic reaction. The samples were integrated with GE, showing a level of electron transportation. The peaks, starting with the highest anodic peak, were as follows: Bare electrode (7.83×10^{-5} ; $-7.75 \times 10^{-5}A$) > QS (7.07×10^{-5} ; $-6.81 \times 10^{-5}A$) > CS-WFM (6.48×10^{-5} ; $-6.34 \times 10^{-5}A$) > AMS (6.02×10^{-5} ; $-6.30 \times 10^{-5}A$) > QF (5.07×10^{-5} ; $-5.53 \times 10^{-5}A$) > AMF (4.87×10^{-5} ; $-5.44 \times 10^{-5}A$).

The lower electrochemical activity peaks for the quinoa and amaranth flour were likely due to the insulating nature of these organic coatings, which hindered the electron transfer diffusion of redox-active species (Ma et al., 2023). Starches primarily comprise polysaccharides (amylose and amylopectin), which are more homogeneous and contain fewer impurities than flours, resulting in higher electrochemical activity peaks than those observed in flours. Flours contain additional components such as proteins, fibers, and lipids, which can introduce more notable insulating effects and complexity to the surface modification, exhibiting smaller electrochemical activity peaks (Patrakova, Gurinovich, Myshalova, & Salishcheva, 2020). The observed higher peak currents with starches compared to flours indicate that starches create a less resistive and obstructive layer on the electrode surface, enabling more efficient electron transfer. The latter behavior of the starches may be closely related to the hydroxyl groups in the free positions of the carbons in the glycosidic bond linkages and pyranose ring formation (Vicentini et al., 2023).

The characterization of these flours and starches targets their use in fermented foods. The diversity in food fermentations results from the various routes and electron acceptors used by microorganisms to balance initial oxidative processes (Hansen, 2018). Additionally, the electrochemical analysis in this study indicated that quinoa flour, amaranth flour, and starches used in products such as fermented sausages may function as electron acceptors. Different acceptors produce diverse metabolic end products, which affect flavor, color, texture, and shelf life (Hansen, 2018).

The charge transfer exhibited by the anodic and cathodic peaks of amaranth and quinoa starches and flours is important in meat products, serving as binders during sausage curing. Controlled oxidation contributes to developing desired flavors and colors in fermented and cured meat products (Bhat, Bhat, & Kumar, 2020). The anodic and cathodic peaks observed in this study indicate that charge transfers enhance starch-protein interactions, thereby stabilising the protein network in meat products such as sausages. This stabilisation extends the shelf life by reducing spoilage rates and improving the texture. Comprehending these interactions enhances processing efficiency, thereby improving the consistency and quality of meat products. Additionally, this inhibits the growth of harmful anaerobic bacteria such as *Clostridium botulinum* while potentially promoting the growth of aerobic microorganisms.

Hu, Ricci, Naranjo, Hill, and Gawason (2021) concluded that electroactive biomaterials (specific proteins and starches) can be used in applications such as nanomedicine, drug delivery, tissue generation, and biosensors owing to their ability to mimic cellular properties. The food industry can potentially leverage these properties, including electrical conduction and electron transfer capacity, for product development using quinoa and amaranth.

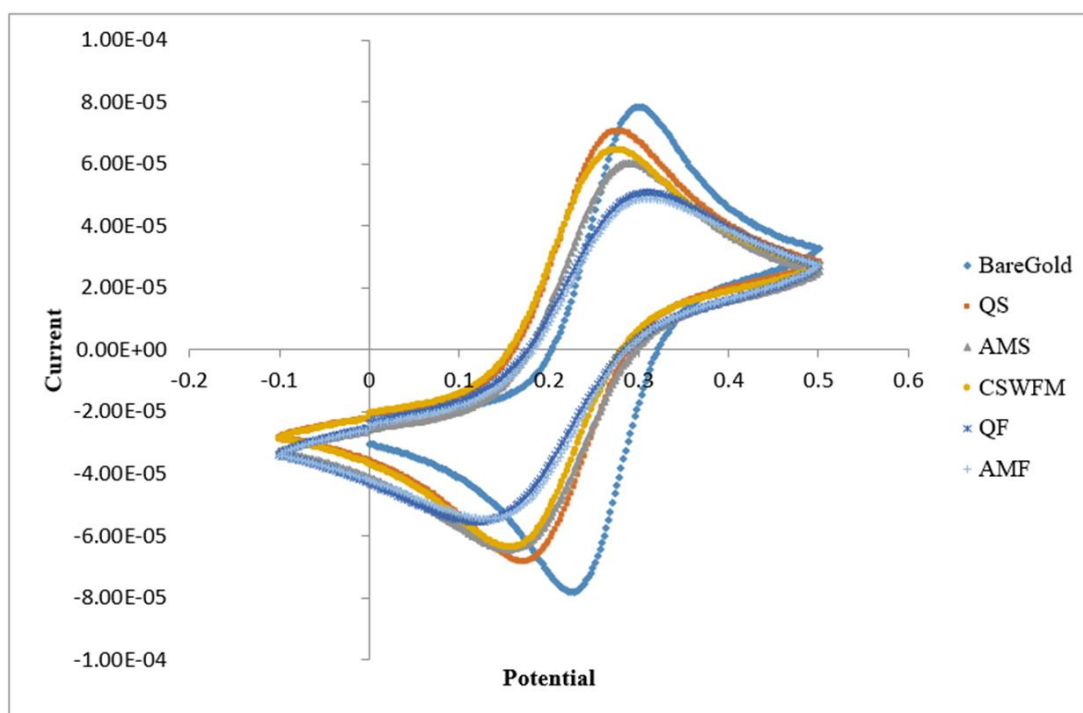


Figure 1. Electrochemical behavior of the ferro/ferricyanide redox couple at the bare GE and modified electrodes with quinoa starch (QS), amaranth starch (AMS), commercial corn starch (CS-WFM), quinoa Flour (QF), and amaranth Flour (AMF).

3.2. Differential Scanning Calorimetry and Thermo Gravimetric Analysis

DSC was used to measure initial gelatinisation, peak gelatinisation temperature, and conclusion temperatures of the flours and starches. Figures 2a and b show the DSC and TGA curves of the samples, respectively. All samples exhibited endothermic peaks associated with starch gelatinisation. The gelatinisation temperature ranged from 31.19°C for corn starch to 51.36°C for amaranth starch. The peak gelatinisation temperature was highest in amaranth flours: AMF (92.70°C) > AMS (90.52°C) > QF (84.83°C) > CS-WFM (83.56°C) > QS (70.41°C). The conclusion temperatures for AMF, AMS, QF, CS-WFM, and QS were 108.13°C, 114.72°C, 98.29°C, 102.60°C, and 103.76°C, respectively (Figure 2a).

The thermal stabilities of the specimens were evaluated using TGA. TGA explains the products' thermal degradation and weight loss characteristics owing to temperature change. All samples showed a mass loss ranging from 25 to 150°C (Figure 2b). Varying degrees of weight loss were observed from 150 to 450 °C, and the total loss recorded for the AMF, AMS, QS, CS, and QF were 84.16%, 77.92%, 88.15%, 87.115%, and 80.19%, respectively. The initial decomposition and peak temperatures were AMF (258.18 °C, 309.98 °C), AMS (249 °C, 307.03 °C), QS (252.20 °C, 311.45 °C), CS (259.06 °C, 307.23 °C), and QF (250.91 °C, 311 °C).

In the present study, the initial gelatinisation temperatures for amaranth flour and starch were lower than those reported by Sindhu and Khatkar (2016). The initial temperatures for amaranth flour were 70.5°C and 108°C, with conclusion temperatures of 82.8°C and 113.7°C (Menegassi, Pilosof, & Arêas, 2011). However, Torres-Vargas et al. (2018) reported peak temperatures as high as 136.5 and 137.5 °C for quinoa and amaranth flour, respectively. Chen et al. (2021) observed a peak temperature of 112 °C for corn starch, which was higher than that observed in this study (83.70°C). Chinnasamy, Dekeba, Sundramurthy, and Dereje (2022) reported an initial temperature of 34.7°C, a peak temperature of 117.9°C, and a conclusion temperature of 179.3°C for corn starch, which were higher than the

temperatures observed in the present study. Rulahnia and Khatkar (2020) reported a higher initial temperature of 50.36°C, a peak temperature of 96.49°C, and a concluding temperature of 146°C for quinoa starch compared to temperatures observed in this study. Temperature differences may be due to variations in analytical methods (Orlova & Aider, 2021). Different samples may exhibit varying capacities to form complexes, such as amylose-lipid complexes, which can alter temperatures. These complexes hinder the swelling and gelatinisation of starch granules, requiring higher temperatures to break down crystalline regions. The marginally higher temperatures observed in this study compared to others could be attributed to proteins interfering with starch water absorption (Sindhu & Khatkar, 2016).

All the samples showed minor mass loss between 25 and 90.8 °C, which was within the reported range of 30 to 150 °C (Xue et al., 2019). Temperatures between 30 and 175 °C are associated with the moisture elimination of light volatiles (Ali, Saeed, Sohail, Aloufi, & Yehia, 2024). The difference may be attributable to free and bound water loss. The second stage (250–312°C) possibly indicates the primary breakdown of starch, resulting in an average mass loss of 45.82% to 64.85%. Aparco, Tadeo, Laime, Ferro, and Camacho (2022) proposed that this temperature range could potentially break down low-molecular-weight peptides. The results are consistent with a previous study by Zhu et al. (2020) who found that starch undergoes thermal deterioration at 280 to 320°C. TGA analysis of quinoa starch revealed a total weight loss of 71.93% from 136.89 to 600°C, which was lower than that observed in the current study. Weight loss that occurred from 150 to 400°C was possibly linked to dietary fibre degradation (Xue et al., 2019). Conversely, the peak decomposition temperature (313.13 °C) was consistent (Ligarda-Samanez et al., 2023). Corn starch analysis showed an initial decomposition temperature of 297°C and a peak decomposition temperature of 316°C (Chen et al., 2021). Chinnasamy et al. (2022) reported an initial decomposition temperature of 284.65°C and a peak of 414.71°C, with a total loss of 89.26%, which is partially consistent with the results obtained in the current study. The differences in decomposition temperatures might be due to the breakdown of organic compounds, lipids, and proteins in corn starch (Aparco et al., 2022).

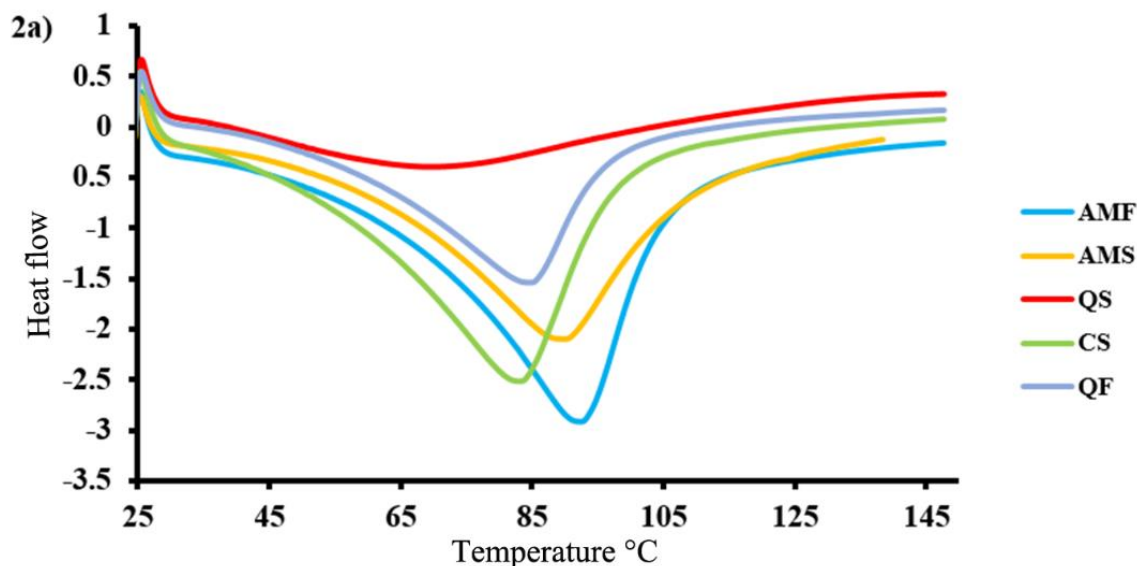


Figure 2a. DSC for AMF, AMS, QS, CS, and QF.

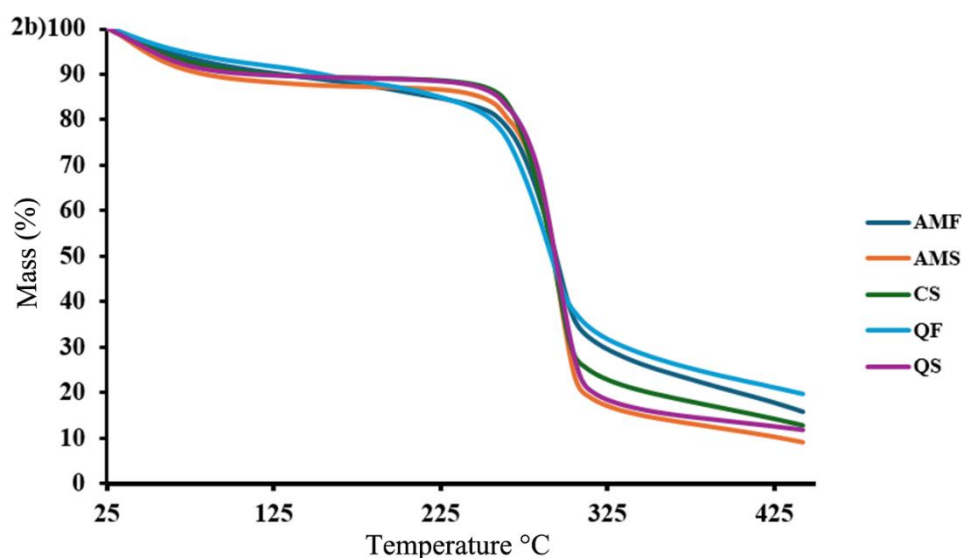


Figure 2b. TGA for AMF, AMS, QS, CS, and QF.

3.3. FTIR

The different types of chemical bonds and functional groups within quinoa starch, amaranth starch, quinoa flour, amaranth flour, and corn starch, and the results are presented in Figure 3. Bands were observed in the O–H region at 3200–3600 cm^{-1} for all the samples. Strong bands were also observed in the region at 1600–1700 cm^{-1} . The flours and starches exhibited bands in the range of 1000–1200 cm^{-1} , with amaranth showing two bands at 1022 and 1153 cm^{-1} . The flours and starches also displayed bands at 600–700 cm^{-1} .

The starches and flours exhibited bands between 1100 and 1153 cm^{-1} , which are associated with C–O–C and C–O–H linkages representing glycosidic bonds found in amylose and amylopectin structures. The C–O–H group contains hydroxyl groups, which enhance the material's hydrophilicity. This is consistent with Peng, Yin, Dong, Shen, and Zhu (2022), who identified a band at 1153 cm^{-1} for quinoa flour, and Jan et al. (2017), who reported bands at 1118 and 1102 cm^{-1} in corn starch and quinoa starch, respectively. However, bands representing similar functional groups were observed in the 1241–1244 cm^{-1} range for amaranth starch (Sindhu & Khatkar, 2016). Additionally, within the 1150–1250 cm^{-1} range, the C–N stretches represented are associated with primary amines and aromatic groups Nandiyanto, Oktiani, and Ragadhita (2019). Torres-Vargas et al. (2018) also observed a C–N bond in quinoa flour. Bands were also observed in the range of 1443–1441 cm^{-1} for all starches and flours except for quinoa flour. The bands indicated C–H bending vibrations of methyl groups, which are components of starch stretches (Peng, Yin, Dong, Shen, & Zhu, 2022). Similar findings for amaranth and corn starch have been reported (Pozo et al., 2018; Sindhu & Khatkar, 2016). Jan et al. (2017) attributed the bands to the angular deformation of the C–H bond in corn and quinoa starch. Bands from 1642 to 1653 cm^{-1} were observed in the flours and starches, potentially indicating tightly bound water in starches, causing H–O–H bending vibrations (Jan et al., 2017; Pozo et al., 2018). Consequently, analogue bands for quinoa, amaranth, and corn starches have been reported (Ligarda-Samanez et al., 2023; Marta, Cahyana, Bintang, Soeherman, & Djali, 2022; Sindhu & Khatkar, 2016). The bands observed in amaranth and quinoa flours might be attributed to a combination of compounds, which include adsorbed water and amine or amide bonds. Siwatch, Yadav, and Yadav (2019) reported a band at 1644 cm^{-1} in amaranth flour, which they attributed to amide II and amide I. Contreras-Jiménez, Torres-Vargas, and Rodríguez-García (2019) demonstrated that a band at 1640 cm^{-1} in quinoa flour represented the amide I bond, indicating the presence of proteins in the flour..

Bands were observed in the range of 3386–3408 cm^{-1} for the starches and flours, indicating the broad O–H bond associated with type A crystallization in starches and flours (Pozo et al., 2018). Sindhu and Khatkar (2016) reported the bond in amaranth starch and attributed it to the O–H stretching of free alcohols and phenols. Additionally, the band at 3389 cm^{-1} in quinoa starch is due to phenolic extracts or phenols (Ligarda-Samanez et al., 2023). Marta et al.

(2022) reported a 3100–3700 cm^{-1} range in corn starch, indicating the O–H bond. Nandiyanto et al. (2019) suggested that bands in flours might be due to the contribution of hydroxyl groups from carbohydrates and proteins.

Amaranth starch was the only sample with a band at 1022 cm^{-1} , which was also reported by Siwatch et al. (2019) in amaranth flour, possibly associated with the amorphous structure of starch. Ligarda-Samanez et al. (2023) reported a similar band at 1021 cm^{-1} in quinoa starch, contradicting the results of the present study. The band at 1024 cm^{-1} was also reported for quinoa flour (Peng et al., 2022). All samples exhibited a band at 657–659 cm^{-1} . In the FTIR spectrum, O–H out-of-plane bending is commonly observed at approximately 650 cm^{-1} , indicating the presence of hydroxyl groups, particularly in carbohydrates and other oxygen-containing organic molecules (Nandiyanto et al., 2019). For quinoa flour and starch, out-of-plane bending might be linked to C–H and O–H groups, especially in polysaccharides and other organic compounds, including alcohols and phenols (Nandiyanto et al., 2019). Consequently, quinoa and amaranth are suitable for use in baked and meat products. In meat products, they enhance the colour and flavour, as well as delay or prevent the oxidation of biomolecules in food, thereby increasing shelf life (Manassis et al., 2020).

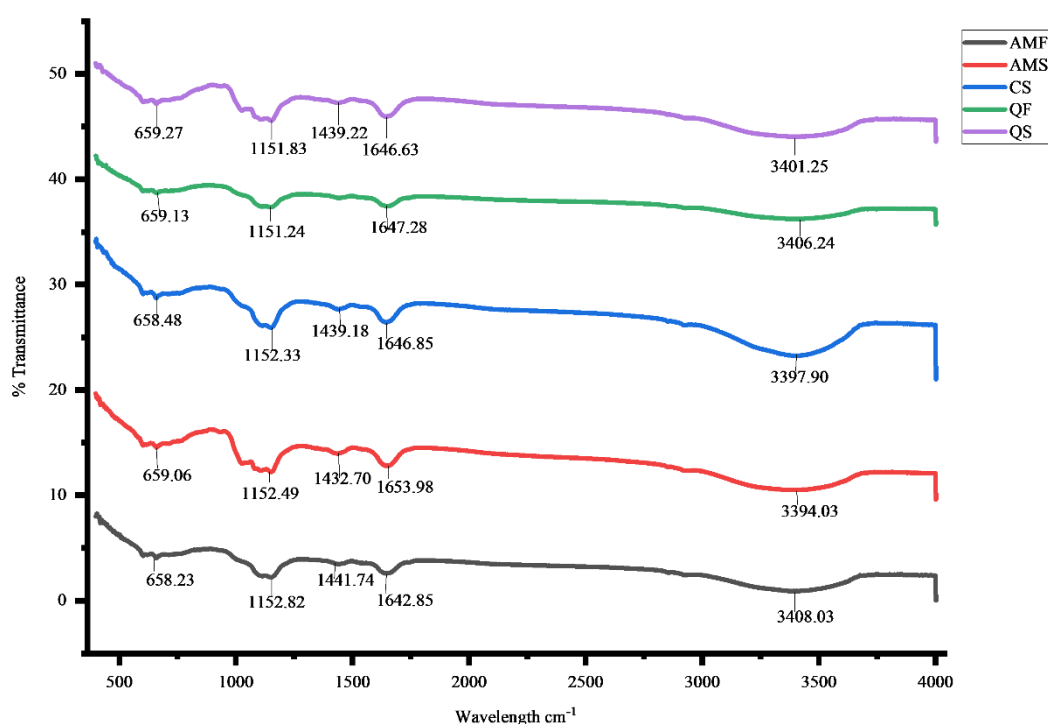


Figure 3. IR spectrum of AMF, AMS, QS, CS-WFM, and QF.

3.4. PXRD

The X-ray diffraction patterns of the flours are shown in Figure 4. The flours and starches had similar diffractograms with strong peaks at 15°, 17°, 18°, and 23°, exhibiting A-type crystalline structures, which correspond to the orthorhombic crystal structure of the Miller indexes (Vega-Rojas et al., 2021). However, quinoa starch and flour had peaks at 26° and 26.3°, respectively. Corn starch, amaranth flour, and quinoa starch exhibited peaks at 19.6°, 20.2°, and 19.5°, respectively, which still fall under the orthorhombic crystalline phase. A peak at 12.9° was also observed in the diffractogram of corn starch, which is not described in the Miller indices.

The highest diffraction peak was observed for the CS-WFM, which had an intact crystalline region, indicating a high crystal content. AMS and AMF sample X-ray diffraction patterns were similar. Relative crystallinity varied between 23.6% and 35.5%, with CS-WFM exhibiting the highest value and AMF showing the lowest value (Table 1).

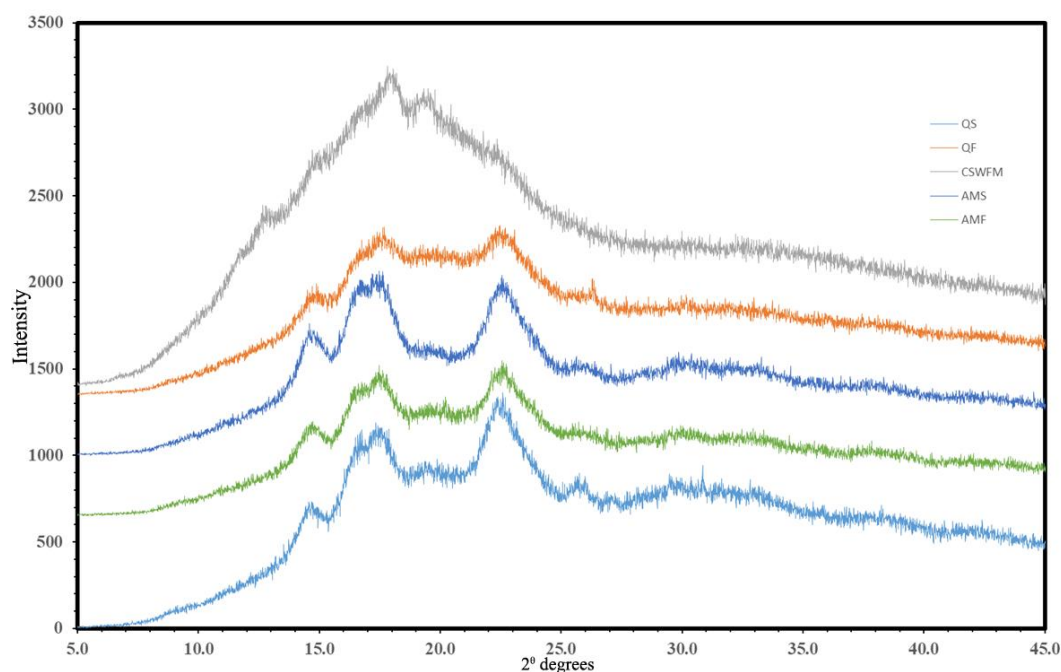


Figure 4. PXRD patterns of AMF, AMS, QS, CS-WFM, and QF.

Table 1. Relative crystallinity of CS-WFM, AMS, QF, QS, and AMF.

Sample	CS-WFM	AMS	QF	QS	AMF
Relative crystallinity	35.5%	31.2%	25.5%	31.4%	23.6%

Note: AMF, amaranth flour; AMS, amaranth starch; QS, quinoa starch; CS-WFM, Commercial corn-starch; QF, quinoa flour.

The flours and starches exhibited a typical A-type pattern, with peaks at $2\theta = 15^\circ$, 17° , 18° , and 23° or within a $\pm 0.5^\circ$ range. These results are consistent with a previous study on A-type starches and flours (Wang, Hu, Zhan, Xu, & Tian, 2020). In contrast, corn starch showed peaks at 12.9° and 19.6° , which indicate the crystalline nature of amylose-lipid complexes in granules (Dong et al., 2021; Kibar, Gönenc, & Us, 2010). Kibar et al. (2010) obtained a percentage crystallinity of 35% for corn starch, which is approximately consistent with 35.5% in the present study. The difference in crystallinity may be attributed to variations in the amylose-amylopectin ratio and the size of crystallites in the corn-starch granules, which can vary depending on the different varieties used (Pérez, Baldwin, & Gallant, 2009; Valdez-Arana et al., 2020).

Quinoa flour and starch had an additional peak at 26.3° . Pozo et al. (2018) reported peaks at 15.05° , 17.09° , 17.92° , 23° , and 26.33° , which were consistent with the findings of this study. The peak at 26° might indicate the presence of SiO_2 (silica), commonly found in flours (Ayala-Landeros et al., 2016). Murphy and Matanguihan (2015) also confirmed the presence of silica in quinoa flours. Quinoa flour had a crystallinity of 25.5%, similar to the 25.1% reported by Dong et al. (2021). The crystallinity of quinoa starch ranged from 21.5% to 43% (Orlova & Aider, 2021). These differences may be attributed to variations in the quinoa varieties analysed (Valdez-Arana et al., 2020).

Amaranth flour peaked at 20.2° , possibly indicating the amylose-lipid complex (Kibar et al., 2010). In this study, the crystallinity of amaranth flour was higher than the 15.27% observed by Siwatch et al. (2019). Amaranth starch had a crystallinity of 31.2%, which was slightly higher than the 20–30% reported by Perez-Rea and Antezana-Gomez (2024). Lower crystallinity percentages are preferred in the development of products such as sausages, as they enhance the high water-binding capacity of the starch, thereby improving characteristics such as texture and mouthfeel (Lourdin et al., 2015).

The crystallinity polymorphs of starch granules are influenced by chain length (CL), the weight average of amylopectin, and amylose content (Jan et al., 2017). The amylopectin molecules of A-type starch have shorter CL (between 23 and 29) (Fuentes et al., 2019). The lower amylose content increases starch crystallinity (Pérez et al.,

2009). Hydration of granules increases crystallinity without altering the original crystal types. Physical properties of starch components, particularly the mole percent of the DP 10–13 short-chain fraction, appear to be more influential in determining crystalline type than the species of origin. The reasons are the relative energies of double helix packing in A and B type starches, the enzymes' inability to handle longer-chain amylopectin, and the disruptive influence of high amylose levels on crystallinity (Cheetham & Tao, 1998).

3.5. UV-Vis Spectrophotometric Fingerprint Analysis

The spectra (Figure 5) showed a wide peak in the range of 340–354 nm for corn starch, which is the standard starch used in most food products. The most prominent peak for corn starch was at 587 nm, within a range of 561–603 nm. Amaranth and quinoa starch had peaks at 337 and 341 nm, respectively. Furthermore, peaks were observed at 740 nm for amaranth flour and starch. Quinoa starch and quinoa flour had prominent bands at wavelengths of 739 and 741 nm, respectively.

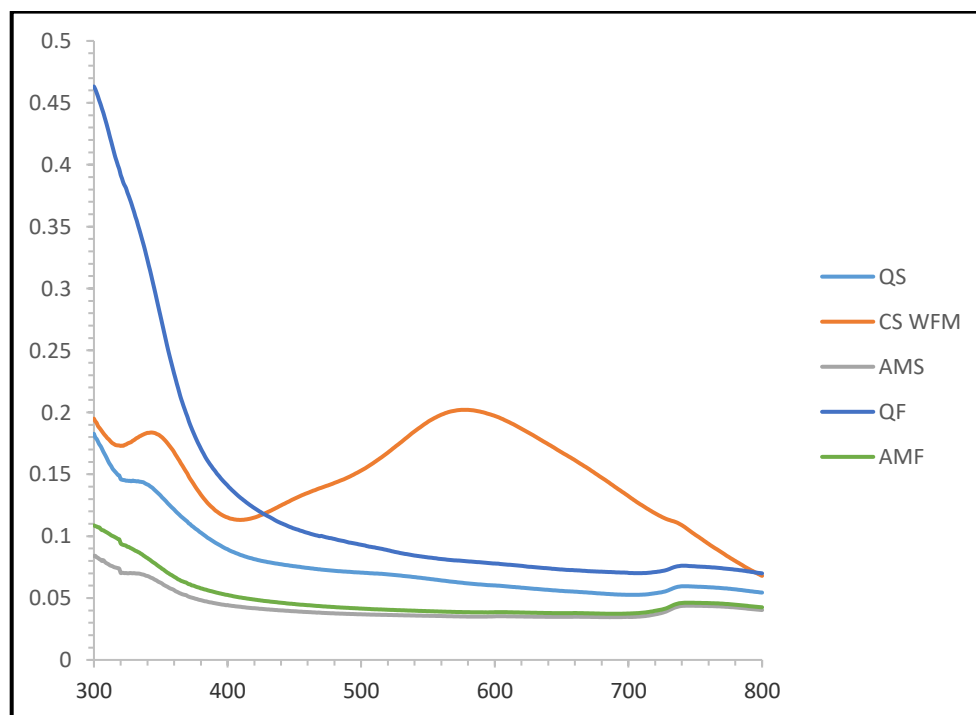


Figure 5. UV-Vis starch spectra of AMF, AMS, QS, CS-WFM, and QF.

The broad peaks observed on corn starch are attributed to starch-iodide complexes (Rundle & French, 1943). Rundle and French (1943) reported that triiodide binding within the amylose helix causes a shift in UV-Vis absorption spectra, with peaks typically at approximately 320–350 nm and in the visible range at approximately 587 nm. The peaks indicate the presence of amylose in the starch, which enhances functional properties such as gel formation and water-binding capacity. These attributes are essential in foods such as sausages or bakery products. Additionally, amylose contributes to retrogradation resistance and digestibility as well as provides nutritional benefits (Ahmad et al., 2021). Pellacani et al. (2023) observed peaks at 609 and 610 nm for corn starch when amylose-iodide complexes formed. However, Moulay (2013) and Sakač et al. (2020) reported starch-iodine complex peaks at 616 and 510 nm for corn starch.

Orlova and Aider (2021) reported a quinoa starch-iodine complex peak range of 587–604 nm, contrary to the present study. Amaranth and quinoa starch, including the flours, did not show any peaks in the ranges reported by Moulay (2013), Sakač et al. (2020), and Pellacani et al. (2023). Peaks for quinoa and amaranth were observed at 341 and 337, respectively, which might be a result of triiodide binding in the amylose helix, as explained by Rundle and

French (1943) or they may be a result of absorption of triiodide ions (Kireev & Shnyrev, 2015). Kireev and Shnyrev (2015) reported that the absorption of triiodide ions ranges from 288 to 350 nm, with a peak at 352 nm. The amylose-iodine complex is commonly characterized, with absorbance measurements typically between 525 and 740 nm (Bahdanovich et al., 2022). Results for quinoa flour, amaranth flour, quinoa starch, and amaranth starch were within the reported range. Several studies optimize the iodine-starch complex method, with wavelengths ranging from 486 to 743 nm for quantification (Bahdanovich et al., 2022). This study supports the findings of Yu, Houtman, and Atalla (1996) who reported ion peaks between 710 and 740 nm owing to iodine ions such as I_{15}^{3-} . Polyiodides in the iodine-amylose complex are occluded in the helical cavity of the amylose and arranged in a linear array parallel to the helical axis (Moulay, 2013). In an amylose-iodine-iodide solution, the polyiodides within the amylose helices exist in equilibrium with iodine and iodide. The wavelength region of the starch-triiodide complex shows noticeable differences, with peaks varying in height and maximum wavelength values owing to the triiodide ion concentration being absorbed by the inner cavities of the helical structures of amylose and amylopectin (Sakač et al., 2020).

However, in this study, the observed peak differences of the materials studied may result from the extraction methods of the starches, which can affect starch concentration and, subsequently, the formation of starch-iodine/iodide complexes. The botanical origin of the material analyzed and specific affinities for triiodide ions may also influence the formation of triiodide ions (Pellacani et al., 2023).

4. CONCLUSION

This study characterized quinoa and amaranth flours and their water-extracted starches, comparing them to corn starch, using electrochemical, thermal, spectroscopic, and X-ray diffraction methods. Electrochemical analysis revealed higher electron transfer efficiency in starches compared to flours, suggesting potential applications in food fermentations. DSC and TGA demonstrated variations in thermal properties related to starch structure and composition. FTIR confirmed the presence of key functional groups. PXRD showed A-type crystalline structures with varying crystallinity, influencing water binding and texture. UV-Vis spectrophotometry revealed distinct spectral fingerprints, with corn starch exhibiting characteristic amylose-iodide complex peaks, while quinoa and amaranth showed different peaks potentially related to triiodide binding. These findings provide valuable insights into the physicochemical properties of these flours and starches, highlighting their potential as functional food ingredients.

Funding: This study received no specific financial support.

Institutional Review Board Statement: Not applicable.

Transparency: The authors state that the manuscript is honest, truthful, and transparent, that no key aspects of the investigation have been omitted, and that any differences from the study as planned have been clarified. This study followed all writing ethics.

Competing Interests: The authors declare that they have no competing interests.

Authors' Contributions: All authors contributed equally to the conception and design of the study. All authors have read and agreed to the published version of the manuscript.

REFERENCES

- Aderibigbe, O., Ezekiel, O., Owolade, S., Korese, J., Sturm, B., & Hensel, O. (2022). Exploring the potentials of underutilized grain amaranth (*Amaranthus* spp.) along the value chain for food and nutrition security: A review. *Critical reviews in Food Science and Nutrition*, 62(3), 656-669. <https://doi.org/10.1080/10408398.2020.1825323>
- Ahmad, M., Rukhsaar, S., Gani, A., Ashwar, B. A., Wani, T. A., Shah, U., & Jhan, F. (2021). Recent advances in the application of starch and resistant starch and slowly digestible starch. In A. Gani & B. A. Ashwar (Eds.), *Food biopolymers: Structural, functional and nutraceutical properties*. In (pp. 59-90). Cham, Germany: Springer International Publishing
- Ali, S. A., Saeed, S. M. G., Sohail, M., Aloufi, A. S., & Yehia, H. M. (2024). Nano-imaging by atomic force microscopy, thermogravimetric characteristics, and bioactive compounds of thermally treated and fermented mash beans. *LWT*, 199, 116131. <https://doi.org/10.1016/j.lwt.2024.116131>

- Aparco, R. H., Tadeo, F. T., Laime, M. D. M. D., Ferro, A. K., & Camacho, J. A. (2022). Thermal behavior in varieties of germinated quinoa (*Chenopodium quinoa* Willd) flour. *Alfa Revista de Investigación en Ciencias Agronómicas y Veterinaria*, 6(16), 130-139. <https://doi.org/10.33996/revistaalfa.v6i16.155>
- Ayala-Landeros, J., Saucedo-Rivalcoba, V., Bribiesca-Vasquez, S., Castaño, V., Martínez-Hernández, A., & Velasco-Santos, C. (2016). Influence of corn flour as pore forming agent on porous ceramic material based mullite: Morphology and mechanical properties. *Science of Sintering*, 48(1), 29-39. <https://doi.org/10.2298/SOS1601029A>
- Bahdanovich, P., Axelrod, K., Khlystov, A. Y., & Samburova, V. (2022). Optimized spectrophotometry method for starch quantification. *Analytica*, 3(4), 394-405. <https://doi.org/10.3390/analytica3040027>
- Balakrishnan, G., & Schneider, R. G. (2022). The role of Amaranth, quinoa, and millets for the development of healthy, sustainable food products—a concise review. *Foods*, 11(16), 2442. <https://doi.org/10.3390/foods11162442>
- Bhat, Z. F., Bhat, H., & Kumar, S. (2020). Cultured meat—A humane meat production system. In Principles of tissue engineering. In (pp. 1369–1388). Cambridge, MA: Academic Press
- Cheetham, N. W., & Tao, L. (1998). Variation in crystalline type with amylose content in maize starch granules: An X-ray powder diffraction study. *Carbohydrate Polymers*, 36(4), 277-284. [https://doi.org/10.1016/S0144-8617\(98\)00007-1](https://doi.org/10.1016/S0144-8617(98)00007-1)
- Chen, X., Yao, W., Gao, F., Zheng, D., Wang, Q., Cao, J., . . . Zhang, Y. (2021). Physicochemical properties comparative analysis of corn starch and cassava starch, and comparative analysis as adhesive. *Journal of Renewable Materials*, 9(5), 979-992. <https://doi.org/10.32604/jrm.2021.014751>
- Chinnasamy, G., Dekeba, K., Sundramurthy, V. P., & Dereje, B. (2022). Physicochemical properties of tef starch: morphological, thermal, thermogravimetric, and pasting properties. *International Journal of Food Properties*, 25(1), 1668-1682. <https://doi.org/10.1080/10942912.2022.2098973>
- Contreras-Jiménez, B., Torres-Vargas, O. L., & Rodríguez-García, M. E. (2019). Physicochemical characterization of quinoa (*Chenopodium quinoa*) flour and isolated starch. *Food Chemistry*, 298, 124982. <https://doi.org/10.1016/j.foodchem.2019.124982>
- Dong, J., Huang, L., Chen, W., Zhu, Y., Dun, B., & Shen, R. (2021). Effect of heat-moisture treatments on digestibility and physicochemical property of whole quinoa flour. *Foods*, 10(12), 3042. <https://doi.org/10.3390/foods10123042>
- FAOSTAT. (2020). *FAOSTAT statistical database*. Rome: Food and Agriculture Organization of the United Nations.
- Fuentes, C., Perez-Rea, D., Bergenstahl, B., Carballo, S., Sjö, M., & Nilsson, L. (2019). Physicochemical and structural properties of starch from five Andean crops grown in Bolivia. *International Journal of Biological Macromolecules*, 125, 829-838. <https://doi.org/10.1016/j.ijbiomac.2018.12.120>
- Hansen, E. B. (2018). Redox reactions in food fermentations. *Current Opinion in Food Science*, 19, 98-103. <https://doi.org/10.1016/j.cofs.2018.03.004>
- Hernandez-Jaimes, C., Lobato-Calleros, C., Sosa, E., Bello-Pérez, L., Vernon-Carter, E., & Alvarez-Ramirez, J. (2015). Electrochemical characterization of gelatinized starch dispersions: Voltammetry and electrochemical impedance spectroscopy on platinum surface. *Carbohydrate Polymers*, 124, 8-16. <https://doi.org/10.1016/j.carbpol.2015.02.002>
- Hu, X., Ricci, S., Naranjo, S., Hill, Z., & Gawason, P. (2021). Protein and polysaccharide-based electroactive and conductive materials for biomedical applications. *Molecules*, 26(15), 4499. <https://doi.org/10.3390/molecules26154499>
- Jan, K. N., Panesar, P., Rana, J., & Singh, S. (2017). Structural, thermal and rheological properties of starches isolated from Indian quinoa varieties. *International Journal of Biological Macromolecules*, 102, 315-322. <https://doi.org/10.1016/j.ijbiomac.2017.04.027>
- Jan, N., Hussain, S. Z., Naseer, B., & Bhat, T. A. (2023). Amaranth and quinoa as potential nutraceuticals: A review of anti-nutritional factors, health benefits and their applications in food, medicinal and cosmetic sectors. *Food Chemistry: X*, 18, 100687. <https://doi.org/10.1016/j.fochx.2023.100687>
- Kibar, E. A. A., Gönenç, I., & Us, F. (2010). Gelatinization of waxy, normal and high amylose corn starches. *GIDA-Journal of Food*, 35(4), 237-244.
- Kireev, S. V., & Shnyrev, S. L. (2015). Study of molecular iodine, iodate ions, iodide ions, and triiodide ions solutions absorption in the UV and visible light spectral bands. *Laser Physics*, 25(7), 075602. <https://doi.org/10.1088/1054-660X/25/7/075602>

- Ligarda-Samanez, C. A., Choque-Quispe, D., Moscoso-Moscoso, E., Pozo, L. M. F., Ramos-Pacheco, B. S., Palomino-Rincón, H., . . . Peralta-Guevara, D. E. (2023). Effect of inlet air temperature and quinoa starch/gum arabic ratio on nanoencapsulation of bioactive compounds from Andean potato cultivars by spray-drying. *Molecules*, 28(23), 7875. <https://doi.org/10.3390/molecules28237875>
- Lourdin, D., Putaux, J.-L., Potocki-Véronèse, G., Chevigny, C., Rolland-Sabaté, A., & Buléon, A. (2015). Crystalline structure in starch. In Y. Nakamura (Ed.), *Starch*. In (pp. 61–90). Tokyo: Springer
- Ma, T., Easley, A. D., Thakur, R. M., Mohanty, K. T., Wang, C., & Lutkenhaus, J. L. (2023). Nonconjugated redox-active polymers: Electron transfer mechanisms, energy storage, and chemical versatility. *Annual Review of Chemical and Biomolecular Engineering*, 14(1), 187–216. <https://doi.org/10.1146/annurev-chembioeng-092220-111121>
- Manassis, G., Kalogianni, A. I., Lazou, T., Moschovas, M., Bossis, I., & Gelasakis, A. I. (2020). Plant-derived natural antioxidants in meat and meat products. *Antioxidants*, 9(12), 1215. <https://doi.org/10.3390/antiox9121215>
- Marta, H., Cahyana, Y., Bintang, S., Soeherman, G. P., & Djali, M. (2022). Physicochemical and pasting properties of corn starch as affected by hydrothermal modification by various methods. *International Journal of Food Properties*, 25(1), 792–812. <https://doi.org/10.1080/10942912.2022.2064490>
- Menegassi, B., Pilosof, A. M., & Arêas, J. A. (2011). Comparison of properties of native and extruded amaranth (*Amaranthus cruentus* L.–BRS Alegria) flour. *LWT-Food Science and Technology*, 44(9), 1915–1921. <https://doi.org/10.1016/j.lwt.2011.04.008>
- Moulay, S. (2013). Molecular iodine/polymer complexes. *Journal of Polymer Engineering*, 33(5), 389–443. <https://doi.org/10.1515/polyeng-2012-0122>
- Murphy, K. S., & Matanguihan, J. (2015). *Quinoa: improvement and sustainable production*. Chichester, UK: John Wiley & Sons.
- Nandiyanto, A. B. D., Oktiani, R., & Ragadhita, R. (2019). How to read and interpret FTIR spectroscopy of organic material. *Indonesian Journal of Science and Technology*, 4(1), 97–118. <https://doi.org/10.17509/ijost.v4i1.15806>
- Noranizan, M., Dzulkifly, M., & Russly, A. (2010). Effect of heat treatment on the physico-chemical properties of starch from different botanical sources. *International Food Research Journal*, 17(1), 127–135.
- Orlova, T., & Aider, M. (2021). Starch grain Quinoa (*Chenopodium quinoa* Willd.): Composition, morphology and physico-chemical properties *Food Processing*, 51(1), 98–112. <https://doi.org/10.21603/2074-9414-2021-1-98-112>
- Patrakova, I., Gurinovich, G., Myshalova, O., & Salishcheva, O. (2020). *Reduction potential of meat, depending on the curing composition*. Paper presented at the International Scientific Conference The Fifth Technological Order: Prospects for the Development and Modernization of the Russian Agro-Industrial Sector (TFTS 2019), Atlantis Press.
- Pellacani, S., Borsari, M., Cocchi, M., D'Alessandro, A., Durante, C., Farioli, G., & Strani, L. (2023). Near infrared and UV-Visible spectroscopy coupled with chemometrics for the characterization of flours from different starch origins. *Chemosensors*, 12(1), 1–18. <https://doi.org/10.3390/chemosensors12010001>
- Peng, M., Yin, L., Dong, J., Shen, R., & Zhu, Y. (2022). Physicochemical characteristics and in vitro digestibility of starches from colored quinoa (*Chenopodium quinoa*) varieties. *Journal of Food Science*, 87(5), 2147–2158. <https://doi.org/10.1111/1750-3841.16126>
- Perez-Rea, D., & Antezana-Gomez, R. (2024). The functionality of pseudocereal starches. In *Starch in food*. In (pp. 377–403). Cambridge, UK: Woodhead Publishing
- Pérez, S., Baldwin, P. M., & Gallant, D. J. (2009). Structural features of starch granules I. In *Starch*. In (pp. 149–192). Cambridge, MA: Academic Press
- Pirzadah, T. B., & Malik, B. (2020). Pseudocereals as super foods of 21st century: Recent technological interventions. *Journal of Agriculture and Food Research*, 2, 100052. <https://doi.org/10.1016/j.jafr.2020.100052>
- Pozo, C., Rodríguez-Llamazares, S., Bouza, R., Barral, L., Castaño, J., Müller, N., & Restrepo, I. (2018). Study of the structural order of native starch granules using combined FTIR and XRD analysis. *Journal of Polymer Research*, 25(12), 266. <https://doi.org/10.1007/s10965-018-1651-y>
- Rulahnia, K., & Khatkar, B. (2020). Isolation and characterization of starch from quinoa (*Chenopodium Quinoa* Willd.). *International Journal of Innovative Research and Advanced Studies*, 7, 1–6.

- Rundle, R., & French, D. (1943). The configuration of starch in the starch—iodine complex. III. X-ray diffraction studies of the starch—iodine complex 1. *Journal of the American Chemical Society*, 65(9), 1707-1710. <https://doi.org/10.1021/ja01249a016>
- Sakač, N., Karnaš, M., Dobša, J., Jozanović, M., Gvozdić, V., Kovač-Andrić, E., . . . Šarkanj, B. (2020). Application of spectrophotometric fingerprinting in cluster analysis to determine the origin of starch. *Food Technology and Biotechnology*, 58(1), 5-11. <https://doi.org/10.17113/ftb.58.01.20.6239>
- Scott, G., & Awika, J. M. (2023). Effect of protein–starch interactions on starch retrogradation and implications for food product quality. *Comprehensive Reviews in Food Science and Food Safety*, 22(3), 2081-2111. <https://doi.org/10.1111/1541-4337.13141>
- Sindhu, R., & Khatkar, B. S. (2016). Characterization of amaranth (*Amaranthus hypocondriacus*) starch. *International Journal of Engineering Research and Technology*, 5(6), 463-469.
- Siwath, M., Yadav, R., & Yadav, B. (2019). Chemical, physicochemical, pasting and microstructural properties of amaranth (*Amaranthus hypocondriacus*) flour as affected by different processing treatments. *Quality Assurance and Safety of Crops & Foods*, 11(1), 3-13. <https://doi.org/10.3920/QAS2017.1226>
- Tang, Y., & Tsao, R. (2017). Phytochemicals in quinoa and amaranth grains and their antioxidant, anti-inflammatory, and potential health beneficial effects: A review. *Molecular nutrition & Food Research*, 61(7), 1600767. <https://doi.org/10.1002/mnfr.201600767>
- Torres-Vargas, O. L., García-Salcedo, Á. J., & Ariza-Calderón, H. (2018). Physicochemical and structural characterization of flours and seeds of quinoa (*Chenopodium quinoa* Willd.), amaranth (*Amaranthus caudatus* L.) and chia (*Salvia hispanica* L.). *Acta Agronomica*, 67(2), 215-223. <https://doi.org/10.15446/acag.v67n2.63666>
- Valdez-Arana, J.-D.-C., Steffolani, M. E., Repo-Carrasco-Valencia, R., Pérez, G. T., & Condezo-Hoyos, L. (2020). Physicochemical and functional properties of isolated starch and their correlation with flour from the Andean Peruvian quinoa varieties. *International Journal of Biological Macromolecules*, 147, 997-1007. <https://doi.org/10.1016/j.ijbiomac.2019.10.067>
- Vega-Rojas, L. J., Alanis-Guzmán, M. G., García-Suárez, F. J., Calderón-Domínguez, G., Ramírez-Wong, B., & Ledesma-Osuna, A. I. (2021). Physicochemical, functional and structural properties of starches isolated from amaranth, quinoa and corn. *Polymers*, 13(15), 2480. <https://doi.org/10.3390/polym13152480>
- Vicentini, F. C., Silva, L. R., Stefano, J. S., Lima, A. R., Prakash, J., Bonacin, J. A., & Janegitz, B. C. (2023). Starch-based electrochemical sensors and biosensors: A review. *Biomedical Materials & Devices*, 1(1), 319-338. <https://doi.org/10.1007/s44174-022-00012-5>
- Wang, Y., Hu, B., Zhan, J., Xu, R., & Tian, Y. (2020). Effects of starchy seed crystals on the retrogradation of rice starch. *Food Chemistry*, 318, 126487. <https://doi.org/10.1016/j.foodchem.2020.126487>
- Xue, Z., Chen, Y., Jia, Y., Wang, Y., Lu, Y., Chen, H., & Zhang, M. (2019). Structure, thermal and rheological properties of different soluble dietary fiber fractions from mushroom *Lentinula edodes* (Berk.) Pegler residues. *Food Hydrocolloids*, 95, 10-18. <https://doi.org/10.1016/j.foodhyd.2019.04.015>
- Yu, X., Houtman, C., & Atalla, R. H. (1996). The complex of amylose and iodine. *Carbohydrate Research*, 292, 129-141. [https://doi.org/10.1016/S0008-6215\(96\)91037-X](https://doi.org/10.1016/S0008-6215(96)91037-X)
- Zhu, L., Wu, G., Cheng, L., Zhang, H., Wang, L., Qian, H., & Qi, X. (2020). Investigation on molecular and morphology changes of protein and starch in rice kernel during cooking. *Food Chemistry*, 316, 126262. <https://doi.org/10.1016/j.foodchem.2020.126262>

Views and opinions expressed in this article are the views and opinions of the author(s), Journal of Food Technology Research shall not be responsible or answerable for any loss, damage or liability etc. caused in relation to/arising out of the use of the content.